Séminaire Poincaré 2 (2004) 39 – 51 **Séminaire Poincaré**

The Quantum Hall Effect as an Electrical Resistance Standard*

B. Jeckelmann and B. Jeanneret
Swiss Federal Office of Metrology and Accreditation
Lindenweg 50
CH-3003 Bern-Wabern
Switzerland

Abstract. The quantum Hall effect (QHE) provides an invariant reference for resistance linked to natural constants. It is used worldwide to maintain and compare the unit of resistance. The reproducibility reached today is almost two orders of magnitude better than the uncertainty of the determination of the ohm in the International System of Units SI. This article is a summary of a recently published review article which focuses mainly on the aspects of the QHE relevant for its metrological application.

1 Introduction

Parallel to the progress made in the physical sciences and in technology, the International System of Units SI has evolved from an artefact based system to a system mainly based on fundamental constants and atomic processes during the last century. The modern units have major advantages over their artefact counterparts: they do not depend on any external parameters like the ambient conditions and, most important, they do not drift with time. In addition they can be simultaneously realized in laboratories all over the world which strongly simplifies and improves the traceability of any measurements to the primary standards.

With the discovery of the Josephson and the quantum Hall effects (QHE), two electrical quantum standards became available. As a first consequence, the worldwide consistency in the realization and maintenance of the electrical units and the electrical measurements based on them has improved hundredfold in the last decade. The two quantum effects will certainly also play a major role in the next modernization of the SI when the last remaining unit in the SI still based on an artefact, the kilogram, will be linked to fundamental constants.

The QHE was discovered on the night of February 5 1980, when Klaus von Klitzing was investigating the transport properties of a Si-MOSFET device at very low temperature and high magnetic field in Grenoble [1]. The discovery, which was totally unanticipated by the physics community, relied on the existence of a two-dimensional electron gas (2DEG) in a semiconducting device. The great technological progress that followed the invention of the transistor lead to the realization of the first 2DEG in semiconducting devices in the middle of the sixties. The first measurements performed with Si-MOSFETs at low temperature and high magnetic field were done by Fowler *et al* [2] in 1966. Later on, due to improvements in device fabrication, Kawaji *et al* [3] observed the dissipationless state in a Si-MOSFET. In 1978, Hall resistance plateaus were observed in such inversion layers by Englert and von Klitzing [4]. However, the idea of analyzing the Hall plateaus in terms of the fundamental value h/e^2 emerged that particular night for the first time. Further measurements [5] confirmed that the fundamental quantization relation for the Hall resistance $R_{\mathrm{H}} = h/ie^2$ was accurate to 10 parts in 10^6. Von Klitzing was awarded the Nobel prize for his discovery in 1985 [6].

The aim of this article is to highlight the role of the QHE in metrology. It summarizes a review article [7] recently published on this subject. Earlier review articles focusing on the metrological aspects of the QHE may be found in [8, 9, 10].

*We thank Institute of Physics Publishing for their kind authorization to reproduce this paper which appeared originally as: *Meas. Sci. Technol.* **14** (2003) 1229-1236; www.iop.org/journals/mst
.

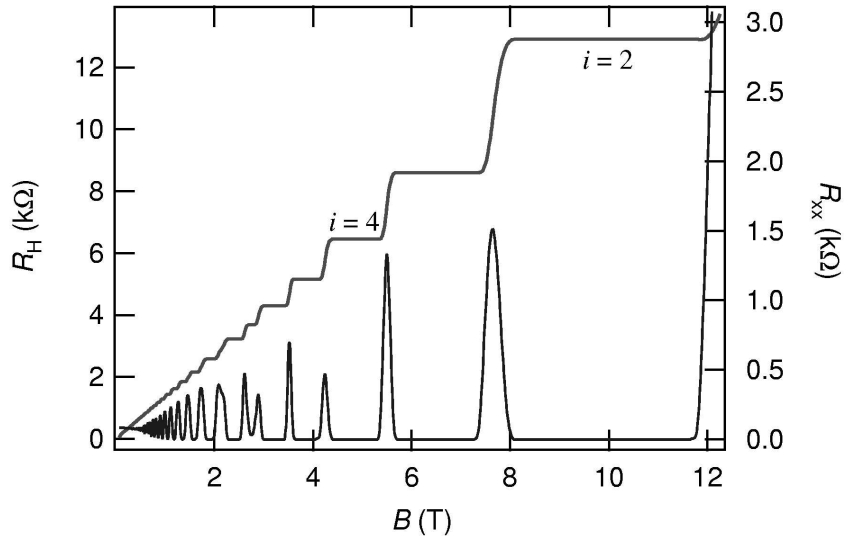

Figure 1: Experimental measurements of the Hall resistance R_{H} and of the longitudinal resistance R_{xx} for a GaAs/AlGaAs heterostructure at a temperature of 0.1 K.

2 Basic Principles

2.1 The Integer Quantum Hall Effect

The QHE is observed in a two-dimensional electron gas at low temperature and high magnetic field. In figure 1, a typical resistance measurement made on a GaAs/AlGaAs sample is shown. A current I flows in the 2DEG of width w, and a longitudinal voltage V_x is measured between two contacts separated by a distance L. At the same time, the transverse voltage V_y is recorded. The voltages and currents are related by

$$V_x = R_{xx} I_x + R_{xy} I_y \tag{1}$$
$$V_y = -R_{xy} I_x + R_{xx} I_y, \tag{2}$$

where R_{xx} is the longitudinal resistance and $R_{xy} = R_{\mathrm{H}}$ is the Hall resistance. In figure 1 broad steps can be observed in the Hall resistance. Simultaneously, the longitudinal resistance vanishes. In a two-dimensional system, the Hall resistance is equal to the Hall resistivity $\rho_{xy} = R_{\mathrm{H}}$. The longitudinal resistance is related to the longitudinal resistivity by $\rho_{xx} = (w/L)R_{xx}$. However, in the quantum Hall regime, $R_{xx} = \rho_{xx} = 0$. Therefore, the resistances are as fundamental as the resistivities in contrast to the three-dimensional case, where geometrical corrections are required. On a plateau, the Hall sample is a perfect conductor with $\rho_{xx} = 0$. However, due to the tensorial nature of the resistance in two dimensions, it is a perfect insulator as well: $\sigma_{xx} = 0$. This can be seen from the relation between the resistivities and the conductivities

$$\rho_{xx} = \frac{\sigma_{xx}}{\left(\sigma_{xx}^2 + \sigma_{xy}^2\right)} \qquad \rho_{xy} = \frac{-\sigma_{xy}}{\left(\sigma_{xx}^2 + \sigma_{xy}^2\right)} \tag{3}$$
$$\sigma_{xx} = \frac{\rho_{xx}}{\left(\rho_{xx}^2 + \rho_{xy}^2\right)} \qquad \sigma_{xy} = \frac{-\rho_{xy}}{\left(\rho_{xx}^2 + \rho_{xy}^2\right)}. \tag{4}$$

A large number of books [11, 12, 13, 14] and review articles [6, 15, 16, 17, 18, 19] is available, which can more deeply introduce the interested readers to the physics of the QHE.

2.2 Landau quantization

The 2DEG needed to observe the QHE can be realized in various types of semiconducting heterostructure devices where the electrons can be confined in a plane. In a high magnetic field, the eigenenergies of the 2D gas of electrons are quantized in so called Landau levels. The unavoidable disorder caused by the impurities present in the system broaden the Landau levels in Landau subbands. A fundamental consequence of the presence of these impurities is to create two different kinds of electronic states: localized and extended states. When the electron density is increased, the various electronic states are gradually filled up. This is equivalent to shifting the Fermi energy E_{F} through the density of states. When E_{F} moves in a mobility gap (region where the electronic states are localized), the occupation of the extended states does not change and, since only these states carry the current, the Hall resistance will not change either, giving rise to a Hall plateau. It is crucial that the energy of the extended states in the middle of this plateaus is well away from E_{F}. In this way, inelastic processes like phonon absorption do not change the occupation of the extended states. Simultaneously to the occurrence of the Hall plateau, the longitudinal resistance vanishes since only localized states are in the vicinity of E_{F}. As soon as E_{F} approaches the next Landau level, dissipation appears in the system and the Hall resistance makes a transition to the next plateau. Therefore, the QHE can be understood as a succession of localization-delocalization transitions when the Fermi energy E_{F} moves across the density of states.

2.3 The edge-state model

An alternative approach to the quantum Hall effect is based on a formalism developed by Landauer [20] where the current is taken as the driving force for the electronic transport rather than an external field. This model [21] takes into account that under quantum Hall conditions a current can flow through the device only if the source and drain contacts are connected by a common edge. The net current is given by the electrochemical potentials of all the terminals and it is the electrochemical potential which is measured in a real experiment at a voltage probe.

For a finite sample width, the Landau levels are bend at the edges of the sample. For each Landau level intercepting the Fermi energy, a one-dimensional channel -called edge channel- is formed. Classically this corresponds to the trajectories of an electron moving along the edge of a device in a magnetic field (skipping orbits).

Büttiker has developed a formalism [21] to describe transport in one-dimensional channels. For the description of the quantum Hall effect, it can be shown that the backscattering in the sample (scattering from one edge to the other) is suppressed and that there is ideal transmission from one contact to the other. Under these conditions it is found that the longitudinal resistance vanishes and the Hall resistance is given by:

$$R_{\mathrm{H}} = \frac{h}{ie^2}. \tag{5}$$

The edge state picture has been successfully used to explain many experiments in connection with the QHE (see e.g.[22] for a review). The model allows a realistic description of the electronic transport in high magnetic fields at least in the domain where the difference in the electrochemical potentials is small compared to the Landau level spacing. For large current densities, however, the current flows mainly in the bulk and an extension of the edge state model is needed to explain the QHE in this regime. However, in metrology the edge-state model is important since it allows a modeling of the contacts.

3 Measurement techniques

Soon after the discovery of the QHE, metrologists started to use the effect as a resistance standard and to study its limitations. For the accurate measurement of resistance, mainly two techniques are in use today: the potentiometric method and the current comparator bridge technique.

The principle of the potentiometric set-up is shown in figure 2. The two resistances R_{H} and R_s to be compared are connected is series and driven by the same dc current source. The voltage

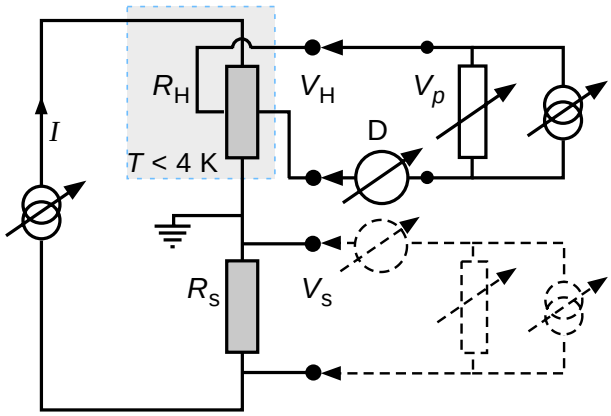

Figure 2: Schematic circuit diagram for a potentiometric resistance bridge. The voltage across the resistors to be compared is closely adjusted against the voltage V_p generated by the potentiometer. The remaining voltage difference is sensed by a high impedance voltage detector.

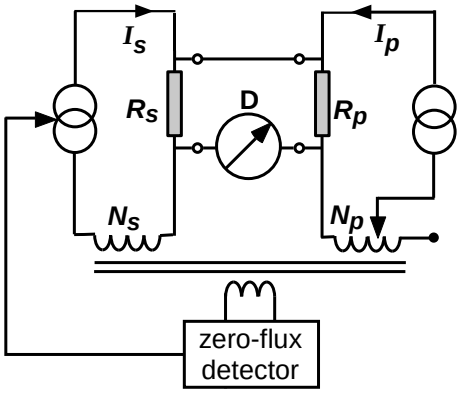

Figure 3: Schematic circuit diagram for a dc current comparator bridge. A servo circuit operating from the output of the magnetometer establishes the zero-flux condition in the magnetic core and accurately sets the current ratio I_p/I_s to the winding ratio N_s/N_p.

drop V_H across R_H is compared against a closely adjusted voltage V_p generated by a potentiometer using a high impedance voltage detector. After this first measurement, V_p and the detector are switched to R_s using a low thermal switch and the second voltage difference $V_s - V_p$ is measured. The difference measurements are repeated for the reversed current polarity. The sequence of current reversals and change of measurement positions is chosen such that linear drifts of the current sources and the thermal voltages are eliminated. The detector D should have a high input impedance and the linearity of the potentiometer has to be checked to allow for a reasonable deviation of the resistance standards from nominal.

A significant improvement of the 1:1 potentiometric bridge is possible by using a Josephson array voltage standard (JAVS) [23] to realize the auxiliary voltage V_p. Modern JAVSs allow the generation of any voltage between 0 V and 10 V. It becomes thus possible to compare e.g. $R_H(2)$ against a 10 kΩ standard. Such measurement systems were first described in [24, 25]. The relative uncertainty reported by the authors was a few parts in 10^8.

Because of the sequential measurements, the potentiometric method is mainly limited by the short term stability of the source. This disadvantage can be eliminated when the two resistance standards to be compared are in two separate current loops which track one another. The set-up of the current comparator bridge is schematically shown in figure 3. The ratio of the two currents is controlled by a dc comparator first realized by Kusters [26, 27]. The two windings N_p and N_s are wound on a high permeability toroidal core. The difference of the magnetomotive

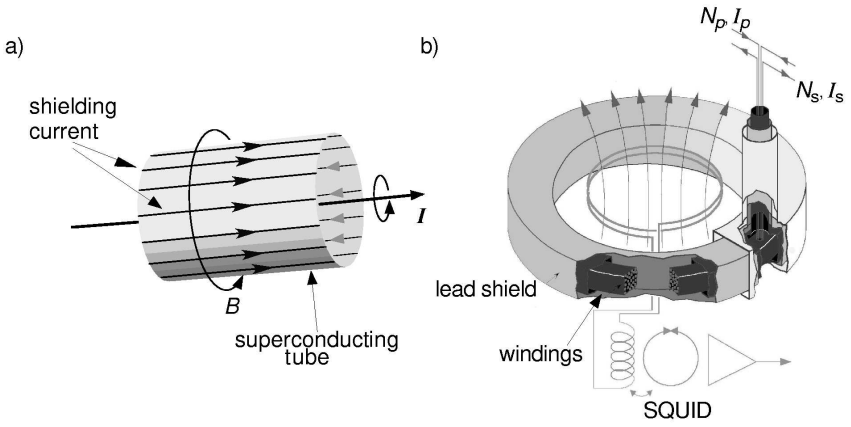

Figure 4: The cryogenic current comparator. (a) Illustration of the principle: a shielding current equal to I is induced on the external surface of the superconducting tube. (b) Set-up of the ratio coils: The windings of the current comparator form a toroidal coil which is enclosed in a superconducting shield. The shield overlaps itself like a snake swallowing its tail. The ampere-turns balance is sensed by measuring the magnetic flux in the pick-up coil using a SQUID.

forces ($N_pI_p - N_sI_s$) can be measured using a second-harmonic flux-gate magnetometer. If an ac modulation is applied to the magnetic core, harmonic components of the modulation are generated if a dc flux is present in the core. A zero-flux condition ($N_pI_p = N_sI_s$) is achieved by means of a servo circuit operating from the output of the magnetometer. Now N_p is adjusted such that the voltage drops across the two resistors R_p and R_s are the same (detector D balanced). Finally, if the flux and voltage balance are met simultaneously, then $R_p/R_s = N_p/N_s$. An accuracy of a few parts in 10^8 can be achieved for the measured ratio.

The best ratio accuracy and the lowest random uncertainty are attained with the cryogenic current comparator (CCC) proposed and first realized by Harvey in 1972 [28]. The principle of the method is shown in figure 4 (a). If a current carrying wire is passed through a superconducting tube, a shielding current is induced on the surface of the tube such that a zero magnetic flux density is maintained in the interior of the superconductor (Meissner effect). The shielding current runs in the same direction as the initial current on the outside of the tube. The current density is uniform over the hole surface and thus independent on the geometrical position of the wire inside the tube. This principle is put in practice in a CCC as illustrated in figure 4 (b). In an arrangement introduced in [29], the superconducting tube is bent to a torus with overlapping ends like a snake swallowing its tail. The overlapping ends are electrically insulated, the length of the overlap has to be > 2 turns to keep the end effects on an acceptable level. Several windings, e.g. N_p and N_s with currents I_p and I_s, respectively, are placed inside the torus. The magnetic flux created by the shielding current on the torus is proportional to $N_pI_p + N_sI_s$. This flux is sensed by a superconducting quantum interference device (SQUID) through a pick-up coil placed in the flux. With a CCC, current ratios $I_s/I_p = N_p/N_s$ with a relative accuracy of 10^{-12} can be realized.

The CCC bridge arrangement is similar to the classical current comparator (figure 3). A stabilized voltage source steers the primary and the secondary current sources. The ratio N_p/N_s of the windings is set as close as possible to the nominal ratio of the two resistors R_p/R_s to be measured. The output voltage of the SQUID system regulates the secondary current source in a closed feedback loop. The resolution of a CCC bridge is mainly given by three factors: The SQUID noise, the thermal noise of the resistors and the detector noise.

Typical parameters for a comparison of the QHR for $i = 2$ ($R_{\mathrm{H}}(2) = 12.9$ kΩ) against a 100 Ω standard are: $N_p = 2065$, $N_s = 16$ and $I_p = 50$ μA. For this configuration, the total rms voltage noise typically amounts to 7 nV/$\sqrt{\mathrm{Hz}}$. It is dominated by the detector noise because R_p is at 1 K. According to this figure, a type-A relative uncertainty of 1 nΩ/Ω is expected within a

measurement time of 2 min. In reality, slightly worse performance is achieved because of $1/f$ noise components (fluctuations of thermal voltages, detector and SQUID).

Today, the lowest uncertainties in resistance comparisons for $1\ \Omega \leq R \leq 100\ \mathrm{k}\Omega$ are obtained using CCC bridges (see e.g. [30, 31, 32, 33]).

4 Universality of the QHR

An incomplete quantization of a plateau due to high current through the device or due to increased temperature leads to a finite ρ_{xx}. A linear relationship exists between the deviation in the measured Hall resistance from the expected value and ρ_{xx}. Finite longitudinal voltages can also be measured as a result of non-ideal contacts. The question is whether the extrapolated value $R_{\mathrm{H}}\left(i, \rho_{xx} \rightarrow 0\right)$ is the same irrespective of the device geometry, material and fabrication process, the carrier mobility and density, the plateau number or other factors. Due to absence of quantitative theoretical models, this question has essentially been approached experimentally.

Already in 1987 an experimental study [34] has shown that the QHRs observed in four different GaAs devices were in agreement at the level of 5×10^{-9}. The search for possible differences between the QHR realized in a GaAs heterostructure and a Si-MOSFET, respectively, was of special interest. In a direct comparison Hartland *et al* [35] found that the difference between the QHR in the two device types was smaller than 3.5 parts in 10^{10}. However, at about the same time, several other groups [36, 37, 38] reported anomalous values of the QHR measured in a particular Si-MOSFET device. The authors claimed to see differences in R_{H} up to several parts in 10^7 despite the absence of any measured dissipation within the experimental resolution. Subsequently, a theoretical model [39] was presented which explains such deviations by the presence of short-range elastic scatterers located at the edges.

A more recent experimental study [40] included devices from the same wafer as those for which the deviant data were obtained. In this case, an agreement between Si-MOSFET and GaAs was found at the level of the experimental uncertainty of 2.3 parts in 10^{10}. The study demonstrated that, due to edge effects, the longitudinal voltage measured along one side of a device can be quite different from the value on the other side. The measurement of zero dissipation at one device side only does, therefore, not guarantee zero V_{xx} values on both sides which is a prerequisite to measure a fully quantized value of R_{H}.

In the same work [40], it was also shown that the extrapolated Hall resistance value $R_{\mathrm{H}}\left(i = 2, 4, \rho_{xx} \rightarrow 0\right)$ does not depend on the device mobility ($13\ \mathrm{T}^{-1} \leq \mu \leq 135\ \mathrm{T}^{-1}$) and the fabrication process (MBE or MOCVD) within 3 parts in 10^{10}.

As for the plateau number i, the results confirm that in GaAs devices no dependence on this quantum number can be seen:

$$\frac{\overline{i \cdot R_H\left(i\right)}}{2 \cdot R_H\left(2\right)} = 1 - \left(1.2 \pm 2.9\right) \cdot 10^{-10},\ i = 1, 3, 4, 6, 8. \tag{6}$$

Among the large number of theoretical papers on the QHE, a few address the question of size effects, including the width dependence of the QHR. Although based on different approaches [41, 42, 43, 44], the majority of these models find that the relative variation of $R_{\mathrm{H}}(i)$ should scale like the inverse square of the device width w, more precisely

$$\frac{\Delta R_{\mathrm{H}}\left(i\right)}{R_{\mathrm{H}}\left(i\right)} = \alpha \left(\frac{l}{w}\right)^2 \tag{7}$$

where $\Delta R_{\mathrm{H}}\left(i\right) = R_{\mathrm{H}}\left(i, w\right) - R_{\mathrm{H}}\left(i, w = \infty\right)$, l is the magnetic length and α is the parameter reflecting the strength of the size effect. In measurements carried out using GaAs Hall bars of widths varying from 10 to 1000 μm [45] no size effect was observed within the experimental uncertainty of 1 part in 10^9. The values for the parameter α are: $(1.8 \pm 1.8)10^{-3}$ and $(0.7 \pm 5.0)10^{-3}$ for the $i = 2$ and $i = 4$ plateau respectively.

These results clearly show that possible size effects are totally negligible for the sample sizes presently used in metrology.

5 The resistance unit in the international system of units SI

The QHE can be used to realize very reproducible resistance values which, to our knowledge, depend only on natural constants. To be used as a practical standard, the value of the QHR has to be known in SI units. In the SI, the electrical units are defined in terms of the mechanical base units metre, kilogram and second through the definition of the ampere and the assumption that electrical power and mechanical power are equivalent. To put the concept of the electrical units in the SI in practice, it is sufficient to realize two electrical units in terms of the m, kg and s. At present, the ohm and the watt are the two chosen units, since they are the most accurately determined.

The realization of the ohm is based on an electrostatics theorem discovered in 1956 by Thompson and Lampard [46]. If we assume an infinitely long conducting pipe of constant cross section in vacuum and divide it into four segments, the theorem states that the cross capacitance per unit length C_1' and C_2' between two opposite segments is given by

$$\exp\left(\frac{-\pi C_1'}{\varepsilon_0}\right) + \exp\left(\frac{-\pi C_2'}{\varepsilon_0}\right) = 1. \tag{8}$$

In a real experiment, the electrodes consist of four cylinders made as symmetrical as possible to make the two cross capacitances C_1' and C_2' agree as closely as possible. The experiment allows the determination of a capacitance change ΔC on the order of 0.1 to 1 pF with a relative uncertainty of <10 nF/F through a single length measurement. Using ac bridge techniques, the capacitance of the calculable capacitor is scaled to a value which can be compared to the resistance of an ac resistor using a quadrature bridge. After proper scaling, this ac resistor is compared to another ac resistor which has a small and calculable ac/dc difference. Dc techniques are finally applied to link the calculable resistor to the QHR.

Despite the long and complicated measurement chain, an accuracy of a few parts in 10^8 is reached using this method [47, 48, 49].

The discovery of the QHE has opened another route for the realization of the ohm. The von Klitzing constant R_K is related with the fine structure constant through the simple relation

$$R_\text{K} \equiv \frac{h}{e^2} = \frac{\mu_0 c}{2\alpha}. \tag{9}$$

In the SI, the permeability of vacuum μ_0 and the speed of light c are fixed quantities with $\mu_0 = 4\pi \times 10^{-7}$ NA^{-2} and $c = 299\ 792\ 458$ m s^{-1}. The fine structure constant can thus be used to determine R_K and test possible corrections to the QHR. Conversely, if R_K is assumed to be identical to $i \cdot R_\text{H}(i)$, the QHE opens up an additional route to the determination of α which does not depend on QED calculations. In figure 5 all the results are shown which contributed to the least square adjustment of α, as given in the 1998 set of fundamental physical constants recommended by the CODATA task group [50].

At present, the most accurate value for α is derived from the anomalous magnetic moment a_e of the electron. A relative experimental uncertainty of 3.7×10^{-9} has been reached so far [50]. A value for the fine structure constant can be obtained from the experimental value of a_e by comparing it to the theoretical value which can be, up to some insignificant correction terms, expressed in the framework of quantum electrodynamics as a power series in α. The most important terms in the series can be calculated analytically, but for some of the higher order terms extensive numerical calculations are necessary [51]. The uncertainty of the theoretical calculation of a_e is estimated to be 1 part in 10^9 [50].

The second most important result taken into account in the calculation of the actual value for α comes from the realization of R_K through the calculable capacitor assuming $R_\text{H}(i = 1) = R_\text{K}$. As the comparison shows, there is no disagreement between the R_K and the a_e derived value for α within the experimental uncertainty.

As we have seen, the best realization of the ohm in the SI is about two orders of magnitude less accurate than the reproducibility of the QHR. A similar situation is found in the case of the volt where the Josephson effect represents a voltage standard which is far more reproducible than

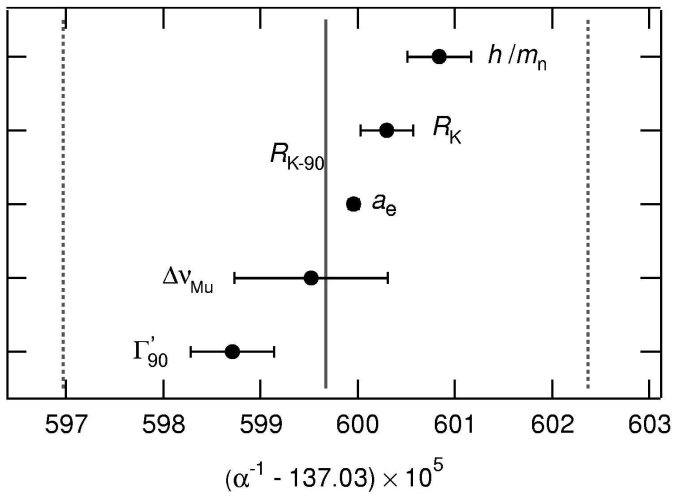

Figure 5: Values for the fine structure constant taken into account in the 1998 adjustment of fundamental constants [50]. The vertical lines indicate the value corresponding to $R_{\text{K-90}}$ and its uncertainty. Γ'_{90} is the value from the measurement of the gyromagnetic ratio of the shielded proton; $\Delta\nu_{\text{Mu}}$ is related to the muonium ground-state hyperfine splitting, a_e to the anomalous magnetic moment of the electron and h/m_n to the ratio of the Planck constant and the neutron mass.

the realization of the SI voltage unit. Two electrical units realized in terms of the non-electrical SI units metre, kilogram and second are needed to make the other electrical units measurable in the SI. With the QHE and the Josephson effect, two fundamentally stable standards are available and thus it was realized the world-wide consistency of electrical measurements could be improved by defining conventional values for R_{K} and for the Josephson frequency to voltage coefficient $K_{\text{J}} \equiv 2e/h$. It was the task of the Comité Consultatif d'Électricité (CCE) to recommend such values based on the data available. All the values for R_{K} and K_{J} available by June 1988 in units of the SI were analyzed and the following conventional values were proposed [52]:

$$\begin{aligned} R_{\text{K-90}} &= 25812.807\,\Omega \\ K_{\text{J-90}} &= 483597.9\ \text{GHz/V}. \end{aligned}$$

Relative uncertainties with respect to the SI of 2×10^{-7} and 4×10^{-7} respectively were assigned to the two values. The conventional values were accepted by all member states of the Metre Convention and came into effect as of January 1, 1990.

In the case of $R_{\text{K-90}}$, the chosen value is essentially the mean of the most accurate direct measurements of R_{K} based on the calculable capacitor and the value from the calculation of the fine-structure constant based on the anomalous magnetic moment of the electron [52]. In the most recent least-square adjustment of fundamental constants carried out by the CODATA Task Group on Fundamental Constants [50], $R_{\text{K}} = 25812.807572\ \Omega$ with a relative uncertainty of 3.7 parts in 10^9 was evaluated. This new value is in good agreement with the conventional value, $R_{\text{K-90}}$. Figure 5 shows the results that were taken into account in the calculation of the new R_{K} value and consequently the new recommended value for α.

5.1 The use of the QHR as a standard of resistance

Since January 1, 1990, most major national metrology institutes are using the QHE to realize a representation of the SI-unit ohm on the basis of the conventional value $R_{\text{K-90}}$. There is overwhelming experimental evidence that the value of R_{K} is independent of the experimental conditions as long as the QHE device is fully quantized. Temperature, current or contact effects may cause deviations from the correct value. Most important, however, test measurements can reveal whether the device is in a proper state or not. This means that the value of the QHR can be made as reproducible as

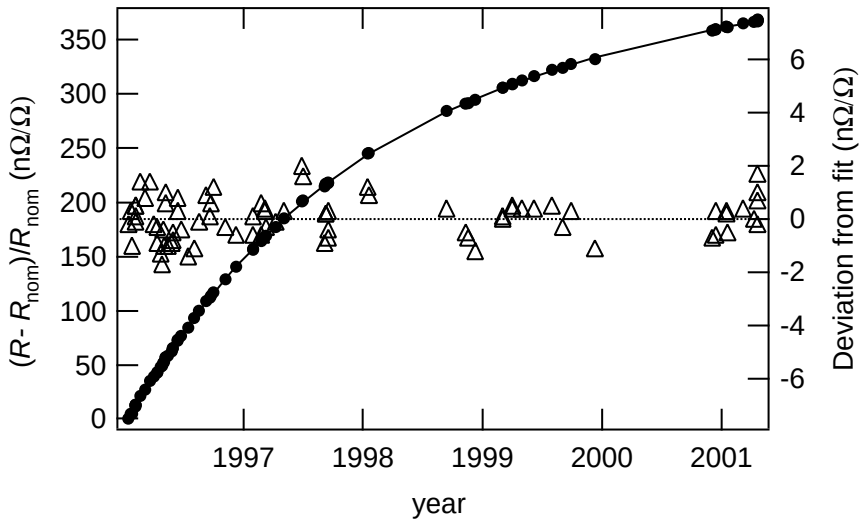

Figure 6: Tracking of a 100 Ω standard resistor measured in terms of $R_{\text{K-90}}$. The triangles (right scale) indicate the deviations of the measured data points to the fit function. Data taken at the Swiss Federal Office of Metrology and Accreditation (METAS).

today's measurement techniques allow without making reference to an external standard. These are the criteria a standard has to fulfill to be accepted as primary standard.

To guarantee the accuracy and reproducibility of the QHR standard, the QHE device, the measurement system and the procedures have to meet a number of strict requirements. A group of experts under the auspices of the CCE has put together the "Technical Guidelines for Reliable Measurements of the Quantized Hall Resistance" [53] which, when correctly applied in practice, assure correct QHR measurements.

The resistance bridges of the type briefly introduced in section 3 are used to calibrate traditional room temperature resistance standards in terms of the QHR. As an example, figure 6 shows the measurements carried out at METAS to determine the drift behavior of a temperature stabilized wire-wound 100 Ω resistor. The standard is kept under constant ambient conditions. As the results show, its resistance can be described with high accuracy by a smooth fitting function, which makes it usable as a transfer standard at the level of 1 nΩ/Ω.

To check the world-wide consistency of the QHR measurements at the highest accuracy level, the BIPM has started in 1993 to perform on-site comparisons of resistance ratio measurements using a transportable QHE standard and resistance bridge. The results of the bilateral comparisons (see e.g. [54]) are made public by the BIPM in a database which is accessible by internet (www.bipm.org). The comparison results obtained so far are shown in figure 7. The agreement between each laboratory and the BIPM for the $R_{\text{H}}(2)/100\ \Omega$ is on the order of one part in 10^9 which is well within the combined standard uncertainty of the comparisons.

6 Conclusion

Many systematic studies have been carried out in the last two decades to assess the accuracy of the QHR. There is now overwhelming experimental evidence that the QHR is a universal quantity. It is independent of host material, device and plateau number at the level of a few parts in 10^{10} which is the resolution of today's measurement techniques. As a consequence, the QHR is used by all the major national metrology institutes as a dc standard for resistance. The reproducibility of this quantum standard is two orders of magnitude better than the absolute realization of the ohm in the SI. By fixing conventional values for the von Klitzing constant R_{K} and the Josephson constant K_{J}, the worldwide consistency of the electrical measurements has improved considerably

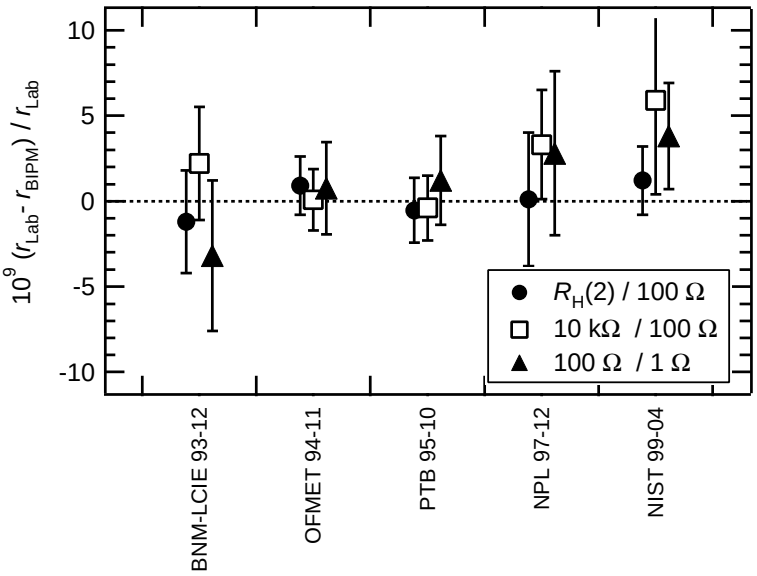

Figure 7: Results of on-site comparisons of three different resistance ratios using the BIPM transportable QHE system.

during the last decade.

Despite the successful application of the QHE in metrology, our understanding of the effect is still incomplete. The many theoretical models explain various aspects of the QHE, at least in a qualitative way. A complete theory which conclusively explains e.g. the remarkable accuracy of the QHR is still missing.

References

[1] G. Landwehr, The discovery of the quantum Hall effect, *Metrologia* **22**, 118–127 (1986).

[2] A.B. Fowler, F.F. Fang, W.E. Howard, and P.J. Stiles, Magneto-oscillatory conductance in silicon surfaces, *Phys. Rev. Lett.* **16**, no. 20, 901–903 (1966).

[3] S. Kawaji, T. Igarashi, and J. Wakabayashi, Quantum galvanometric effect in n-channel silicon inversion layers under strong magnetic fields, *Prog. Theor. Phys. Suppl.* **57**, 176–186 (1975).

[4] T. Englert and K. von Klitzing, Analysis of ρ_{xx} minima in surface quantum oscillations on (100) n-type silicon inversion layers, *Surf. Sci.* **73**, 70–80 (1978).

[5] K. von Klitzing, G. Dorda, and M. Pepper, New method for high-accuracy determination of the fine structure constant based on quantized Hall resistance, *Phys. Rev. Lett.* **45**, no. 6, 494–497 (1980).

[6] K. von Klitzing, The quantized Hall effect, *Rev. Mod. Phys.* **58**, no. 3, 19–531 (1986).

[7] B. Jeckelmann and B. Jeanneret, The quantum Hall effect as an electrical resistance standard, *Rep. Prog. Phys.* **64**, 1–53 (2001).

[8] M. Cage, *The quantum Hall effect*, ch. Experimental aspects and metrological applications, pp. 37–67. Springer Verlag, 2nd edition, 1990.

[9] A. Hartland, The quantum Hall effect and resistance standards, *Metrologia***29**, 175–190 (1992).

[10] T.J. Witt, Electrical resistance standards and the quantum Hall effect, *Rev. Sci. Instrum.* **69**, no. 8, 2823–2843 (1998).

[11] R.E. Prange and S.M. Girvin, eds., *The Quantum Hall Effect, 2nd edition.* Springer-Verlag, New-York, 1990.

[12] H. Kamimura and H. Aoki, *The Physics of Interacting Electrons in Disordred Systems.* Oxford University Press, New York, 1989.

[13] M. Janssen, O. Viehweger, U. Fastenrath, and J. Hajdu, *Introduction to the Theory of the Integer Quantum Hall Effect.* VCH Verlagsgesellschaft, Weinheim, 1994.

[14] T. Chakraborty and P. Pietilainen, *The Quantum Hall Effect*, vol. 85. Springer-Verlag, New-York, 1995.

[15] T. Ando, A.B. Fowler, and F. Stern, Electronic properties of two-dimensional systems, *Rev. Mod. Phys.* **54**, no. 2, 437–672 (1982).

[16] H. Aoki, Quantised Hall effect, *Rep. Prog. Phys.* **50**, 655–730 (1987).

[17] D.R. Yennie, Integral quantum Hall effect for nonspecialists, *Rev. Mod. Phys.* **59**, no. 3, 781–824 (1987).

[18] S. Kawaji, Quantum transport in semiconductors surface and interface channels, *Surf. Sci.* **299/300**, 563–586 (1994).

[19] B. Huckestein, Scaling theory of the integer quantum Hall effect, *Rev. Mod. Phys.* **67**, no. 2, 357–396 (1995).

[20] R. Landauer, Electrical resistance of disordered one-dimensional lattices, *Philos. Mag.***21**, 863–867 (1970).

[21] M. Büttiker, Absence of backscattering in the quantum Hall effect in multiprobe conductors, *Phys. Rev. B* **38**, no. 14, 9375–9389 (1988).

[22] R.J. Haug, Edge state transport and its experimental consequences in high magnetic fields, *Semicond. Sci. Techno.* **8**, 131–153 (1993).

[23] C.A. Hamilton, C.J. Burroughs, and K. Chieh, Operation of NIST Josephson array voltage standard, *J. Res. Nat. Inst. Stand. Technol.* **95**, no. 3, 219–235 (1990).

[24] T. Endo, Y. Murayama, M. Koyanagi, J. Kinoshita, K. Inagaki, C. Yamanouchi, and K. Yoshihiro, Measurement system for quantum Hall effect utilizing a Josephson potentiometer, *IEEE Trans. Instrum. Meas.* **34**, no. 2, 323–327 (1985).

[25] P. Warnecke, J. Niemeyer, F.W. Dünschede, L. Grimm, G. Weimann, and W. Schlapp, High-precision resistance ratio measurements by means of a novel Josephson potentiometer, *IEEE Trans. Instrum. Meas.* **36**, no. 2, 249–251 (1987).

[26] N.L. Kusters, W.J.M. Moore, and P.N. Miljanic, A current comparator for precision measurements of dc ratios, *IEEE Trans. Commun. Electron.* **83**, 22–27 (1964).

[27] M.P. MacMartin and N.L. Kusters, A direct-current comparator ratio bridge for four-terminal resistance measurements, *IEEE Trans. Instrum. Meas.* **15**, no. 4, 212–220 (1966).

[28] I.K. Harvey, Precise low temperature dc ratio transformer, *Rev. Sci. Instrum.* **43**, 1626–1629 (1972).

[29] D.B. Sullivan and R.F. Dziuba, Low temperature direct current comparators, *Rev. Sci. Instrum.* **45**, no. 4, 517–519 (1974).

[30] J.M. Williams and A. Hartland, An automated cryogenic current comparator resistance ratio bridge, *IEEE Trans. Instrum. Meas.* **40**, no. 2, 267–270 (1991).

[31] F. Delahaye and D. Bournaud, Low-noise measurements of the quantized Hall resistance using an improved cryogenic current comparator bridge, *IEEE Trans. Instrum. Meas.* **40**, no. 2, 237–240 (1991).

[32] R.F. Dziuba and R.E. Elmquist, Improvements in resistance scaling at NIST using cryogenic current comparators, *IEEE Trans. Instrum. Meas.* **42**, no. 2, 126–130 (1993).

[33] B. Jeckelmann, W. Fasel, and B. Jeanneret, Improvements in the realisation of the quantized Hall resistance standard at OFMET, *IEEE Trans. Instrum. Meas.* **44**, no. 2, 265–268 (1995).

[34] F. Delahaye and D. Dominguez, Precison comparison of quantized Hall resistances, *IEEE Trans. Instrum. Meas.* **36**, no. 2, 226–229 (1987).

[35] A. Hartland, K. Jones, J.M. Williams, B.L. Gallagher, and T. Galloway, Direct comparison of the quantized Hall resistance in gallium arsenide and silicon, *Phys. Rev. Lett.* **66**, no. 8, 969–973 (1991).

[36] S. Kawaji, N. Nagashima, N. Kikuchi, J. Wakabayashi, B.W. Ricketts, K. Yoshihiro, J. Kinoshita, K. Inagaki, and C. Yamanouchi, Quantized Hall resistance measurements, *IEEE Trans. Instrum. Meas.* **38**, no. 2, 270–275 (1989).

[37] C.T. van Degrift, K. Yoshihiro, M.E. Cage, D. Yu, K. Segawa, J. Kinoshita, and T. Endo, Anomalously offset quantized Hall plateaus in high-mobility Si-MOSFETs, *Surf. Sci.* **263**, 116–119 (1992).

[38] K. Yoshihiro, C.T. van Degrift, M.E. Cage, and D. Yu, Anomalous behavior of a quantized Hall plateau in a high-mobility Si metal-oxide-semiconductor field-effect transistor, *Phys. Rev. B* **45**, no. 24, 14204–14214 (1992).

[39] O. Heinonen and M.D. Johnson, Failure of the integer quantum Hall effect without dissipation, *Phys. Rev. B* **49**, no. 16, 11230–11237 (1994).

[40] B. Jeckelmann, B. Jeanneret, and D. Inglis, High precision measurements of the quantized Hall resistance: Experimental conditions for universality, *Phys. Rev. B* **55**, no. 19, 13124–13134 (1997).

[41] A.H. MacDonald and P. Středa, Quantized Hall effect and edge currents, *Phys. Rev. B* **29**, no. 4, 1616–1619 (1984).

[42] B. Shapiro, Finite-size corrections in the quantum Hall effect, *J. Phys. C* **19**, 4709–4721 (1986).

[43] W. Brenig and W. Wysokinski, Scattering approach to the von Klitzing effect, *Z. Phys. B* **63**, 149–154 (1986).

[44] R. Johnston and L. Schweitzer, An alternative model for the integral quantum Hall effect, *Z. Phys. B* **72**, 217–224 (1988).

[45] B. Jeanneret, B. Jeckelmann, H.J. Bühlmann, R. Houdré, and M. Ilegems, Influence of the device width on the accuracy of quantization in the integer quantum Hall effect, *IEEE Trans. Instrum. Meas.* **44**, no. 2, 254–257 (1995).

[46] A.M. Thompson and D.G. Lampard *Nature (London)*, **177**, 2–88 (1956).

[47] A.M. Jeffery, R.E. Elmquist, L.H. Lee, J.Q. Shields, and R.F. Dziuba, NIST comparison of the quantized Hall resistance and the realization of the SI ohm through the calculable capacitor, *IEEE Trans. Instrum. Meas.* **46**, no. 2, 264–268 (1997).

[48] G.W. Small, B.W. Rickets, P.C. Coogan, B.J. Pritchard, and M.M.R. Sovierzoski, A new determination of the quantized Hall resistance in terms of the NML calculable cross capacitor, *Metrologia* **34**, 241–243 (1997).

[49] A. Hartland, R.G. Jones, B.P. Kibble, and D.J. Legg, The relationship between the SI ohm, the ohm at NPL, and the quantized Hall resistance, *IEEE Trans. Instrum. Meas.* **36**, no. 2, 208–213 (1987).

[50] P.J. Mohr and B.N. Taylor, CODATA recommended values of the fundamental physical constants: 1998, *Rev. Mod. Phys.* **72**, no. 2, 351–495 (2000).

[51] T. Kinoshita, The fine structure constant, *Rep. Prog. Phys.* **59**, 1459–1492 (1996).

[52] B.N. Taylor, Basic standards and fundamental constants, *IEEE Trans. Instrum. Meas.* **38**, no. 2, 164–166 (1989).

[53] F. Delahaye, Technical guidelines for reliable measurements of the quantized Hall resistance, *Metrologia* **26**, 63–68 (1989).

[54] F. Delahaye, T.J. Witt, B. Jeckelmann, and B. Jeanneret, Comparison of quantum Hall effect resistance standards of the OFMET and the BIPM, *Metrologia* **32**, 385–388 (1996).